Eur. Phys. J. B **42**, 423–429 (2004)
DOI: 10.1140/epjb/e2004-00399-x

THE EUROPEAN PHYSICAL JOURNAL B

Stability analysis of fronts in a tristable reaction-diffusion system

E.P. Zemskov and K. Kassner[a]

Institut für Theoretische Physik, Otto-von-Guericke-Universität, Universitätsplatz 2, 39106 Magdeburg, Germany

Received 4 November 2003 / Received in final form 9 August 2004
Published online 23 December 2004 –

Abstract. A stability analysis is performed analytically for the tristable reaction-diffusion equation, in which a quintic reaction term is approximated by a piecewise linear function. We obtain growth rate equations for two basic types of propagating fronts, monotonous and nonmonotonous ones. Their solutions show that the monotonous front is stable whereas the nonmonotonous one is unstable. It is found that there are two values of the growth rate for the most dangerous modes (corresponding to the longest possible wavelengths), $\omega = 0$ and $\omega < 0$, for the monotonous front, so that at $\omega = 0$ the perturbation eigenfunction is positive whereas when $\omega < 0$ it changes sign. It is also noted that the eigenvalue $\omega = 0$ becomes negative in an inhomogeneous system with a particular (stabilizing) inhomogeneity. Counting arguments for the number of eigenmodes of the linear stability operator are presented.

PACS. 05.45.-a Nonlinear dynamics and nonlinear dynamical systems – 47.20.Ma Interfacial instability – 47.54.+r Pattern selection; pattern formation

Reaction-diffusion equations have been studied extensively and for a long time as a qualitative model for nerve conduction [1]. The dynamics are usually taken to be excitable and describe pulse solutions. The study of equations with another basic type of the dynamics describing fronts has also a long history going back to the works of Fisher [2] and Kolmogorov, Petrovskii and Piskunov [3]. The simplest reaction-diffusion equation describing a front connecting two stable fixed points (the rest and the excited states) has a cubic nonlinearity and is called bistable model [4]. In the present paper, our interest is directed at a generalization of the bistable model to a multistable case. Fronts in a multistable reaction-diffusion equation may be considered as composed of bistable fronts [5]. Such compositions may produce monotonous or nonmonotonous solutions. We will consider here a simple multistable model – a tristable equation, where a quintic nonlinear reaction term is approximated by a piecewise linear function. This approach, well-known in the literature [6–14], allows us to obtain analytic solutions for the propagating waves. The method has more general applicability and is often the only way to investigate some nonlinear problems analytically in an approximate fashion [15]. In most papers related to reaction-diffusion equations, bistable [8,10,14] and excitable [7,9,11] systems are investigated. However, to the best of our knowledge, before the present study, no fully analytic solutions of the stability problem for monotonous and nonmonotonous tristable fronts were available. In reference [16], the global stability of monotonous fronts was investigated only. Thus, the problem statement for our work is the linear stability analysis of basic front types in a piecewise linear tristable equation.

Piecewise linear approximations of the reaction terms use the Heaviside step function $\theta(u)$, so that using this approach the tristable equation can be written as

$$\frac{\partial u(x,t)}{\partial t} = -u - 1 + \theta(u-\eta) + \theta(u-\eta^*) + \frac{\partial^2 u(x,t)}{\partial x^2}, \quad (1)$$

where η and η^* are constants, $|\eta|, |\eta^*| < 1$, for definiteness $\eta^* > \eta$. This equation admits two basic types of propagating fronts[1]. The first front solution interpolates from $u = -1$ as $\xi \to -\infty$ to $u = 1$ as $\xi \to \infty$ and consists of three pieces (monotonous 3-front). The second solution connects $u = -1$ and $u = 0$ passing through all three zones. This front consists of four pieces (nonmonotonous 4-front). To construct the front solutions one imposes the matching conditions for the functions and their derivatives at matching points ξ_0, ξ_0^* (and ξ_0^{**} for the 4-front), where adjacent parts of the solution are patched together. Due to translational invariance of the basic equations, the position of one matching point can be chosen arbitrarily, for example, $\xi_0 = 0$. This is a consequence of the homogeneity of the model. In Figure 1, we give an example of both solutions. The obtained fronts have different velocities and shapes. For a given reaction-diffusion system, the speed of the 4-front is larger than that of the 3-front. Velocity dependences will be presented and discussed below. The

[a] e-mail: kassner@physik.uni-magdeburg.de

[1] One introduces traveling frame coordinate $\xi = x - ct$, where c is the front velocity. Then equation (1) transforms to an ODE for $u(\xi)$.

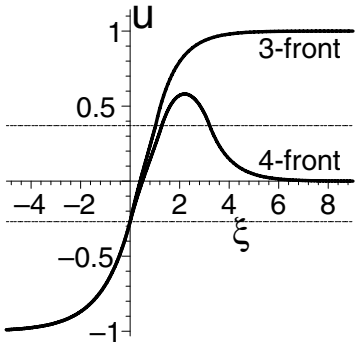

Fig. 1. Monotonous (3-front) and nonmonotonous (4-front) traveling waves. The dashed lines represent the boundary values η and η^*, restricting middle interfacial zones of the fronts.

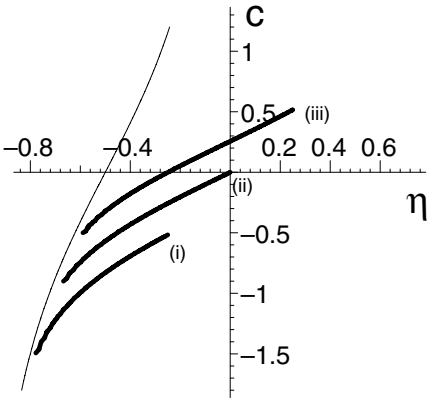

Fig. 2. Velocity behavior described by equation (2) in the homogeneous model for the monotonous front (thick curves), c versus η, for different values of η^*: (i) $\eta^* = -1/4$, (ii) $\eta^* = 0$ and (iii) $\eta^* = 1/4$. The thin curve corresponds to the asymptotics $\lambda^+ + \gamma\eta = 0$.

shape of the waves is determined by the positions of the matching points ξ_0, ξ_0^* and ξ_0^{**}. The first matching point, $\xi_0 = 0$, is the same for both waves and the second matching points do not differ significantly. The crucial factor is the appearance of a third matching point in the 4-front profile that is responsible for a hump in the wave shape. However, this is still a front, not a combined front-pulse wave, because the initial and the final states are different. In the bistable front, there is no hump in the wave profile. A hump can appear in the case of nonlocal equations (with an integral convolution in space) [17]. The hump of the 4-front grows in the ξ direction when the value of the second boundary η^* increases (at fixed η). Then the value of the third matching point ξ_0^{**} grows faster than the value ξ_0^*. However, there exists a restriction [18] on the size of the zone between η and η^*. Mathematically, the restriction condition arises due to a second matching point occuring, which can be observed during the derivation of the front velocity relationship. Its appearance, though not its precise form, may be conveniently discussed in terms of a mechanical analogue, provided by a particle in a triple-hill potential [4], formed by integration of the reaction term in equation (1). The potential is piecewise parabolic and the front speed is identified with a friction coefficient.

The simplest case is that of a steady front, where the friction coefficient is zero. Then the left and right maximum have to be of the same height for the 3-front to exist *and* the middle maximum has to be lower. For the 4-front, the particle starts from the position $u = -1$, passes through the point $u = 0$, but does not reach $u = 1$, instead it comes back to $u = 0$. So for a steady 4-front to exist, the right maximum must be higher than the other two, which have to be of the same height.

For nonzero front velocities and, hence, friction coefficients, a 3-front can in principle exist, if the three maxima form a monotonously decreasing or increasing sequence. Consider the case of positive friction (i.e., front velocity). Then the particle in the potential may move from $u = -1$ to $u = 0$, still having a positive velocity and come to rest on the maximum at $u = 1$, which may be lower than that at $u = 0$, because the particle still loses energy while going from $u = 0$ to $u = 1$. However, it should be clear that there is a restriction on the height of the third maximum; if the latter is too low, the particle will overshoot and, hence, a front solution does not exist.

4-fronts with positive speed (corresponding to a positive friction coefficient) can exist only, if the middle maximum of the triple-hill potential is lower than the other two. For if the right maximum were *not* higher than the middle one, a particle returning because it did not reach the energy of the maximum at $u = 1$ would not be able to end up on the maximum at $u = 0$.

This discussion shows that for certain arrangements of the triple-hill potential a 3-front may exist while a 4-front is impossible. In general, if the middle maximum is lower than the two outer ones, both fronts will exist. A similar discussion may of course be carried through for negative front velocities.

As earlier in the bistable model, the front speed may be determined from the matching conditions. Reducing the number of equations via elimination of all unknowns except the velocity, we obtain a relationship for the latter. In the case of the 3-front it reads [18]

$$\frac{1}{\lambda^+}\ln\left(\frac{-\lambda^-}{\lambda^+ + \gamma\eta}\right) = \frac{1}{\lambda^-}\ln\left(\frac{-\lambda^- - \gamma\eta^*}{\lambda^+}\right) = \xi_0^*, \quad (2)$$

where $\lambda^\pm = -c/2 \pm \sqrt{c^2/4 + 1} \equiv (-c \pm \gamma)/2$. Hence it follows that $\eta = -\eta^*$ in the case of zero velocity, i.e., when the piecewise linear function representing the reaction part of equation (1) is symmetric about zero, the 3-front is stationary. The velocity behavior described by equation (2) is shown in Figure 2. The thick curves display front speed curves, c versus η, for different values of η^*. When $\eta^* < 0$ the velocity is negative for any value of η [curves (i) and (ii) in Fig. 2]. For positive η^*, the velocity may be positive or negative depending on the position of η [curve (iii)]. The speed increases as the distance $\eta^* - \eta$ decreases, so that the maximum value of c on each speed

curve occurs at vanishing size of the middle interfacial zone of the front profile[2] when $\eta^* \to \eta$. When this zone grows, the speed curve tends to an asymptotic line (thin curve), described by the equation $\lambda^+ + \gamma\eta = 0$. A similar behavior (speed growth with η^*) is observed for the c versus η^* dependences at different values of η. In the last case, the asymptotics is $\lambda^- + \gamma\eta^* = 0$. Both asymptotics are derived from equation (2) and the fact that $\pm\lambda^\pm > 0$.

In the case of the 4-front, the procedure of the velocity determination is mathematically the same, and we turn our attention to the discussion of the speed behavior. For a symmetric reaction term, the velocity of the 4-front is nonzero, as opposed to the 3-front wave. The explanation of this result is provided by the particle-in-a-potential analogy again. Due to the symmetry, the left and right hills are global maxima whereas the middle one is only a local maximum. The particle representing the 4-front should return to the (lower) middle maximum, which it can do only for a positive friction, i.e. positive front speed.

Next we explore the problem of the traveling front stability. To perform the stability analysis, we consider a perturbed solution of the form $u(\xi) + \tilde{u}(\xi)\mathrm{e}^{\omega t + \mathrm{i}py}$, where the wave number p is fixed and the growth rate $\omega(p)$ is a function of the wave number. The tristable equation differs from the bistable model only in the number of the Heaviside functions. Therefore, as in the bistable case, ω and p appear in the equation in the combination $\omega + p^2$, i.e., the fastest growing mode will then always be at $p = 0$ and we may restrict ourselves to the $p = 0$ case as long as we are interested in global stability only. The details of the stability analysis for the 3-front are collected in the Appendix, where the growth rate relationship

$$(\Omega\chi - 1)(\Omega\chi^* - 1) = \mathrm{e}^{-\Omega\xi_0^*} \tag{3}$$

is obtained. Here, we have introduced the notation $\Omega = \sqrt{c^2 + 4(1+\omega)}$. The parameters

$$\chi = \left|\frac{du}{d\xi}\Big|_{\xi_0}\right| = \lambda^+(1+\eta) \;\text{ and }\; \chi^* = \left|\frac{du}{d\xi}\Big|_{\xi_0^*}\right| = -\lambda^-(1-\eta^*) \tag{4}$$

are calculated at both matching points for the unperturbed front solutions $u(\xi)$, taking into account that the parameters $|\eta|, |\eta^*| < 1$ and $\pm\lambda^\pm > 0$. The relationship (3) is depicted in Figure 3 as $\omega = \omega(\eta)$ for different values of η^*. For each η^* the diagram demonstrates two lines that present $\omega = 0$ and $\omega < 0$ solutions. Both lines terminate at some value of η. This magnitude corresponds to a limited boundary value for the size of the middle zone obtained from the above mentioned restriction [18]. When the value η^* grows, both lines in Figure 3 shift to the right side on the diagram, but the behavior remains the same. Thus, we conclude that inside some interval of η the 3-front is stable and outside there exists no solution at all.

[2] This zone corresponds to the distance in u between the two points $u = \eta, \eta^*$, i.e., this is also the middle zone in the reaction function $f(u) = 0$.

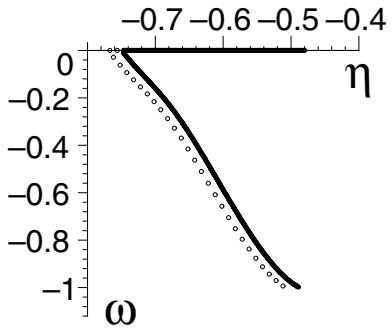

Fig. 3. Growth rate ω of disturbances versus η dependence described by equation (3) for the monotonous 3-front for different values of η^* in the homogeneous model. The solid line corresponds to the solution with speed dependence (iii) in Figure 2 at $\eta^* = 0.25$, whereas the circles present the case $\eta^* = 0.23$.

We note in passing that the transformation $v = \exp(-c\xi/2)\tilde{u}$ turns the variational equation (A.2) into

$$\frac{\partial^2 v}{\partial\xi^2} + [(\delta(u-\eta) + \delta(u-\eta^*)]\, v = \left(1 + \omega + \frac{c^2}{4}\right) v\,,$$

which after introducing the replacements $\delta(u-\eta) = \delta(\xi-\xi_0)/|u'(\xi_0)|$ and $\delta(u-\eta^*) = \delta(\xi-\xi_0^*)/|u'(\xi_0^*)|\,\{+\delta(\xi-\xi_0^{**})/|u'(\xi_0^{**})|\}$, with the term in braces absent for the 3-front and present for the 4-front[3], becomes a one-dimensional time-independent Schrödinger equation with a potential consisting of a sum of two or three δ functions, respectively, and an energy eigenvalue equal to $E = -(1 + \omega + \frac{c^2}{4})$. Since we know that the eigenvalues of a Schrödinger equation are real, we need not consider the possibility of complex values of ω, i.e., we can be sure that there is no Hopf bifurcation and that to determine the front stability, it is sufficient to check where ω changes sign instead of just the real part of ω.

In addition, the transformation to a known Schrödinger equation provides us with information about the multiplicity of possible eigenvalues. First, it is clear that a front has an infinite spectrum, since there is an infinity of possible wave numbers p for the perturbation. However, we have restricted ourselves to just one value of p (namely, $p = 0$) and are now in a position to discuss how many eigenvalues should be expected for each p. It is known that the Schrödinger equation in one dimension with a (negative) δ function potential always has one bound state. This ground state does not have any nodes. If we add a second (negative) δ function potential, the number of bound eigenstates depends on the separation and strength of these δ peaks. Provided they are far enough from each other, a second

[3] To convert the δ function with argument u into one with argument ξ, we have to sum over all zeros of its total argument. There is one root for each δ function if the front profile is monotonous. In the case of the 4-front, there are two roots for $u = \eta^*$.

eigenfunction is possible that changes sign once and has a node between the two peaks. If they are too close to each other, we just stay with a single bound state. Note that only bound states can correspond to positive growth rates in our case, since a positive value of ω implies a negative energy. However, if ω is negative and smaller than $1 + c^2/4$ in absolute value, we still have a bound state. Unbound states of the Schrödinger equation do not decay to zero at infinity and hence do not correspond to legitimate solutions of the stability problem. With a third δ function appearing, we expect a third eigenvalue generically, depending on the distance of the peaks of the potential.

To summarize, we expect up to two eigenvalues for ω in the case of the 3-front and up to three in the case of the 4-front. There will be always one eigenvalue at least, and if there should be only one, this must be $\omega = 0$, since the translational mode is neutral in the basic homogeneous model of equation (1).

Using equation (4) and the expressions for $\lambda^{\pm}$, we find that $\chi = \chi^*$ yields $-2c + c(\eta^* - \eta) + \gamma(\eta^* + \eta) = 0$. Hence in the case of a stationary front ($\eta^* = -\eta, c = 0$), the growth rate relationship (3) is reduced to

$$2(1+\eta)\sqrt{1+\omega} - 1 = \pm(1+2\eta)^{\sqrt{1+\omega}}. \qquad (5)$$

To determine the critical points $\eta_{\rm crit}$, where the stability behavior changes (in the general case ω changes sign, in our case the solution disappears), we set $\omega = 0$ in equation (5). Then we obtain the equivalence (identity) at any η for the plus sign and $\eta = -1/2$ for the minus sign on the right side of equation (5). Thus, there is a trivial $\omega = 0$ solution of equation (5) for any value of $\eta \in (-1/2, 0)$. The relationship (5) may be depicted as $\omega = \omega(\eta)$ as was done for equation (3) in Figure 3. The obtained diagram shows again two lines with $\omega = 0$ and $\omega < 0$ similar to Figure 3. Each line corresponds to a solution of equation (5) with a different sign on the right side. The equation with the positive sign yields the straight line at $\omega = 0$ and the case with the negative sign describes the curve at $\omega < 0$. Both lines terminate at $\eta_{\rm crit} = -1/2$, i.e., the motionless 3-front is stable inside the interval between $\eta = -1/2$ and $\eta = 0$[4] (which is its entire existence interval). The trivial case $\omega = 0$ makes sense, because the solution should have translational invariance. Indeed, if translational invariance is violated, for example, due to an inhomogeneity in the model equation, then in the growth rate relationship additive terms related to the particular solution $\bar{u}(\xi)$ of the inhomogeneous problem appear and equation (3) transforms to

$$(\Omega\chi - 1)(\Omega\chi^* - 1) = \mathrm{e}^{\Omega(\xi_0 - \xi_0^*)}. \qquad (6)$$

Here, the value of ξ_0 is essential (it cannot be chosen arbitrarily) since translational invariance does not hold. Of course, now we have a modified velocity relationship [18]

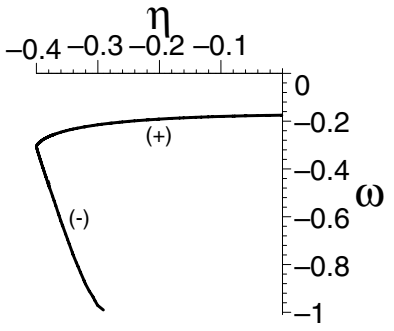

Fig. 4. Growth rate ω versus η dependence for the stationary 3-front in the inhomogeneous model with symmetric reaction term, $\eta^* = -\eta$. The (+) and (−) lines correspond to the solutions of equation (9) with positive and negative signs in the right side, respectively. The coordinates of the termination point are $\eta_{\rm crit} = -0.4$ and $\omega(\eta_{\rm crit}) \approx -0.3$ (the curves are shown for $\xi_0 = 1$ and $f_0 = 0.1$).

$$\frac{1}{\lambda^+}\ln\left[\frac{-\lambda^-}{\lambda^+ + \gamma\eta - \gamma\bar{u}(\xi_0)}\right] = \frac{1}{\lambda^-}\ln\left[\frac{-\lambda^- - \gamma\eta^* + \gamma\bar{u}(\xi_0^*)}{\lambda^+}\right] = \xi_0^* - \xi_0, \qquad (7)$$

where the reaction term constants η, η^* are shifted in comparison with equation (2) due to the particular solution $\bar{u}(\xi)$ of the inhomogeneous problem, $\eta \to \eta - \bar{u}(\xi_0), \eta^* \to \eta^* - \bar{u}(\xi_0^*)$. The jump parameters χ and χ^*,

$$\chi = \left|\lambda^+[1 + \eta - \bar{u}(\xi_0)] + \frac{d\bar{u}(\xi_0)}{d\xi}\right|,$$
$$\chi^* = \left|-\lambda^-[1 - \eta^* + \bar{u}(\xi_0^*)] + \frac{d\bar{u}(\xi_0^*)}{d\xi}\right| \qquad (8)$$

also contain derivatives, $d\bar{u}/d\xi$. Thus, when $\bar{u}(\xi)$=const., the stability behavior remains the same as in the homogeneous system. The only difference is the shift of the termination point, $\eta_{\rm crit} \to \eta_{\rm crit} - \bar{u}$.

To be more specific, let us consider the stationary front ($c = 0$) in the model with symmetric reaction term ($\eta^* = -\eta > 0$) and a linear inhomogeneity, $\bar{f}(\xi) = f_0\xi, f_0 = \mathrm{const} > 0$.[5] Then $\bar{u}(\xi)_{c=0} = f_0\xi$ and the growth rate equation (6) becomes

$$2(1+\eta-f_0\xi_0+f_0)\sqrt{1+\omega}-1 = \pm(1+2\eta-2f_0\xi_0)^{\sqrt{1+\omega}}. \qquad (9)$$

The dependence ω versus η described by equation (9) is presented graphically in Figure 4. The old solution $\omega = 0$ for any η related to the plus sign on the right side of equation (5) disappears here due to the $\bar{u}(\xi)$ inclusions, so that

[4] Since $\eta^* = -\eta$ and $\eta^* > \eta$ the parameter η must be negative.

[5] The positive slope f_0 here is essential to provide only two matching points in the front profile.

the old line $\omega = 0$ is now shifted to the region of negative values of ω. This curve corresponds to the solution of equation (9) with a plus sign on the right side [line (+) in Fig. 4], whereas the equation with a minus sign still describes a curve $\omega < 0$ [line (-)]. The whole behavior ω versus η remains basically the same as compared with Figure 3, only the termination point at $(\eta_{\rm crit}, \omega_{\rm crit})$ for both curves is shifted to larger values of η as follows directly from equation (9): $\eta_{\rm crit} \to \eta_{\rm crit} - f_0\xi_0$, $f_0\xi_0 > 0$. Its coordinates may be obtained by setting to zero each side of equation (9). So, $\eta_{\rm crit} = -1/2 + f_0\xi_0$ and $\omega_{\rm crit} = 1/(1+2f_0)^2 - 1$. Thus, we can summarize that the solution $\omega = 0$ disappears in the inhomogeneous system, in general. For the linear ramp, both ω eigenvalues are negative, so that the 3-front remains still stable. A similar situation is present in the inhomogeneous bistable two-component system. The linear inhomogeneity in space breaks the translational symmetry of both bistable fronts and renders them stable when the slope of f_0 is large [19–21]. When the slope decreases, instability of the front occurs through bifurcation [19,20] if the medium is excitable.

Let us now turn our attention again to the homogeneous system. The solutions for the perturbation eigenfunction $\tilde{u}(\xi)$ and for the perturbed fronts (at $t = 0$) $U(\xi) = u(\xi) + \tilde{u}(\xi)$, are shown in Figure 5 for the symmetric case ($\eta^* = -\eta = 0.4$). The curves $\tilde{u}(\xi)$ and $U(\xi)$ show two bends at $\xi_0 = 0$ and ξ_0^* due to the jumps in the $\tilde{u}$ derivative. As this is a consequence of the piecewise-linear approximation of the reaction term, we suppose that there are no bends in the case of the continuous (quintic) tristable model. The perturbation eigenfunctions $\tilde{u}(\xi)$ can be different in shape. From the expressions for the constants $\tilde{A}_{21}$ and $\tilde{A}_3$ (see Appendix), it follows that when the magnitude $\Omega\chi - 1$ is positive, the perturbation is *always* positive also and has two hills (Fig. 5a). When this magnitude is negative, the perturbation may take on negative values and is hill-well shaped (Fig. 5b). From our analogy with a Schrödinger equation, we realize that in this second case the perturbation eigenfunction has a node and hence must therefore have a negative as well as a positive part. Taking into account equation (5), we conclude that the perturbation is always positive (rather of one sign, because the prefactor is arbitrary) when $\omega = 0$, whereas when $\omega < 0$, the perturbation will have negative values. Again, this is expected from the analogy, as the larger eigenvalue $\omega = 0$ corresponds to the lower energy, i.e., the ground state, of the Schrödinger equation. This result is true for the nonsymmetric case as well.

In the case of the 4-front, the general form of the perturbation eigenfunctions is similar and the matching conditions consist of 9 equations. Omitting the details we write the growth rate equation

$$\Gamma_1\Gamma_2\Gamma_3 \mathrm{e}^{\tilde{\lambda}^+\xi_0^*}\mathrm{e}^{\tilde{\lambda}^-\xi_0^*}\mathrm{e}^{\tilde{\lambda}^+\xi_0^{**}} = (2+\Gamma_2)\mathrm{e}^{\tilde{\lambda}^+\xi_0^*}\mathrm{e}^{\tilde{\lambda}^-\xi_0^*}\mathrm{e}^{\tilde{\lambda}^-\xi_0^{**}} + \Gamma_1\mathrm{e}^{2\tilde{\lambda}^+\xi_0^*}\mathrm{e}^{\tilde{\lambda}^-\xi_0^{**}} + \Gamma_3\mathrm{e}^{2\tilde{\lambda}^-\xi_0^*}\mathrm{e}^{\tilde{\lambda}^+\xi_0^{**}} \quad (10)$$

with $\tilde{\lambda}^\pm = -c/2 \pm \sqrt{c^2/4 + 1 + \omega} \equiv (-c \pm \Omega)/2$, $\Gamma_i = (\Omega\chi_i - 1), i = 1,2,3$, $\chi_1 \equiv \chi, \chi_2 \equiv \chi^*$ and $\chi_3 = |u'(\xi_0^{**})|$. Performing the numeric computation of the growth rate ω in equation (10), we obtain three values $\omega < 0, \omega > 0$ and $\omega = 0$ for each choice η (for the sake of simplicity we restrict ourselves here to the case when $\eta^* = -\eta$). Again, the multiplicity three is expected from the Schrödinger equation analogy. (However, we would expect it to go down to two when ξ_0^* and ξ_0^{**} become almost equal.) Thus, one can make the inference that the 4-front is unstable. We think that the situation closely resembles that in more complex N-fronts (they intersect the line $u = \eta^*$ $N-2$ times in the tristable model), which behave very much like the 4-front. Conditions for the existence of such a kind of generalized front solutions are determined by the corresponding matching equations.

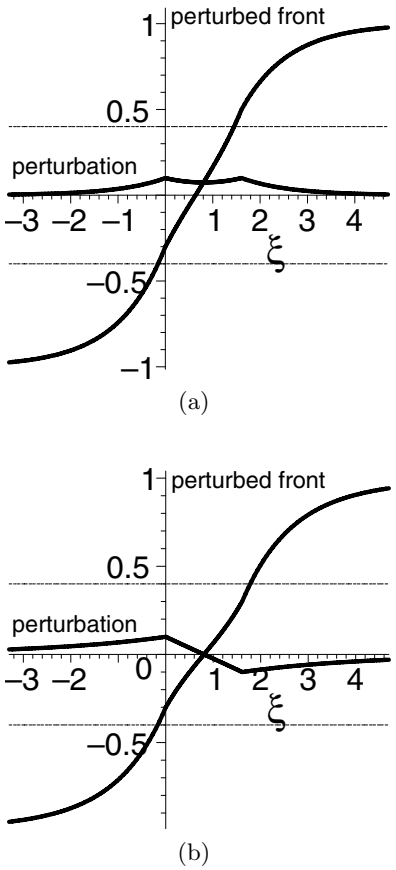

Fig. 5. Perturbation $\tilde{u}(\xi)$ and perturbed motionless monotonous fronts $U(\xi) = u(\xi) + \tilde{u}(\xi)$ at $t = 0$ in the homogeneous model in the cases (a) $\omega = 0$ and (b) $\omega < 0$. The dashed lines are $u = \eta$ and $u = \eta^*$, as in Figure 1.

The analysis presented here applies globally in the model parameter space and may be extended to the general multistable system. Our studies bring up an interesting theoretical question: What is the effect of the 4-front instability, can this unstable front transform to the stable 3-front or to the simple 2-front (bistable front between $u = -1$ and $u = 0$) during its evolution (relaxation to the rest from the perturbed wave)? To answer this question in the affirmative, we would have to investigate the conditions for the existence of a phase transition caused by

the instability of the metastable state. And if these conditions allow the transition between the 4 and 3 or 2-fronts, then the next intriguing question arises: What is the physical mechanism responsible for this transition? For one example, in non-dissipative systems the parametric resonance underlies the mechanism responsible for phase transitions [22]. It is possible that the treatment with reaction-diffusion systems would not strongly violate this principle because the traveling front solutions of the nonlinear Klein-Gordon equation with $u^4 - u^6$ self-coupling considered in reference [22] are similar to the reaction-diffusion fronts. Thus, the stability analysis of the tristable fronts presented here is of great practical importance in nonequilibrium physics applications as the starting point for the development of a nonlinear analysis of the fronts in the multistable models.

In conclusion, a piecewise linear tristable reaction-diffusion equation was investigated. Matching procedures and the stability analysis of fronts were performed analytically. Exact analytic solutions were obtained for the front velocity and the growth rate of perturbations. Two basic types of the tristable fronts, monotonous and non-monotonous (the 3 and 4-fronts), were considered. It was shown that the 3-front is stable and the 4-front is unstable. It is anticipated that similar behavior arises for the combined compositions of tristable fronts. However, we expect more complex behaviour in the case of two-component systems, because in this situation front solutions in the bistable system differ not only in their internal structure but also in their propagation direction, so that the velocity diagrams show a pitchfork bifurcation [23]. The stability analysis presented here can be extended to the case of two-component system, too. Related to the bifurcation diagram we expect similar stability characteristics to be found as in the bistable system.

This work was supported by the *Deutsche Forschungsgemeinschaft* under Grant *FOR 301/2-1 (3)* in the framework of a research group on "Interface dynamics in pattern forming processes".

Appendix: Stability of the 3-fronts in the homogeneous system

A full perturbed solution has the form $U(\xi,t) = u(\xi) + \Delta u(\xi,t)$, where a small perturbation $\Delta u(\xi,t)$ is added to the planar front solution $u(\xi)$. In the frame moving at velocity c, the variational equation for the small perturbation Δu reads

$$\frac{\partial \Delta u}{\partial t} = \frac{\partial^2 \Delta u}{\partial \xi^2} + c\frac{\partial \Delta u}{\partial \xi} + \frac{df(u)}{du}\Delta u. \qquad \text{(A.1)}$$

With a perturbation of the form $\Delta u(\xi,t) = \tilde{u}(\xi)\mathrm{e}^{\omega t}$ and the expression for the reaction term $f(u) = -u - 1 + \theta(u-\eta) + \theta(u-\eta^*)$, it becomes

$$\frac{d^2\tilde{u}}{d\xi^2} + c\frac{d\tilde{u}}{d\xi} - [1 + \omega - \delta(u-\eta) - \delta(u-\eta^*)]\tilde{u} = 0, \quad \text{(A.2)}$$

where $\delta(u)$ is the Dirac delta function. Here we consider the system when ω has positive or small negative values, so that $1 + \omega > 0$. The procedure for the 3 and 4-fronts is essentially the same and we illustrate the analysis only for monotonous wave. Satisfying the boundary conditions $\tilde{u}_1(\xi \to -\infty) = 0$ and $\tilde{u}_3(\xi \to +\infty) = 0$, the solution for the perturbation eigenfunction reads

$$\begin{aligned}
\tilde{u}_1(\xi) &= \tilde{A}_1 \mathrm{e}^{\tilde{\lambda}^+ \xi}, \quad \xi \le \xi_0, \\
\tilde{u}_2(\xi) &= \tilde{A}_{21}\mathrm{e}^{\tilde{\lambda}^+ \xi} + \tilde{A}_{22}\mathrm{e}^{\tilde{\lambda}^- \xi}, \quad \xi_0 \le \xi \le \xi_0^*, \\
\tilde{u}_3(\xi) &= \tilde{A}_3 \mathrm{e}^{\tilde{\lambda}^- \xi}, \quad \xi \ge \xi_0^*,
\end{aligned} \qquad \text{(A.3)}$$

where $\tilde{\lambda}^{\pm} = -c/2 \pm \sqrt{c^2/4 + 1 + \omega} \equiv (-c \pm \Omega)/2$. The perturbation matching conditions differ from the front matching only in the equations for the derivative of $\tilde{u}(\xi)$. Due to the δ-functions in equation (A.2), $d\tilde{u}(\xi)/d\xi$ has finite jump discontinuities at $\xi = \xi_0$ and $\xi = \xi_0^*$. In the matching conditions, there are two small constants, $\tilde{u}_0$ and $\tilde{u}_0^*$, fixing the perturbation eigenfunction. Setting $\xi_0 = 0$ and inserting solution (A.3) into the matching conditions, we obtain a set of equations

$$\begin{aligned}
\tilde{A}_1 &= \tilde{A}_{21} + \tilde{A}_{22}, \\
\tilde{A}_1\tilde{\lambda}^+ &= \tilde{A}_{21}\tilde{\lambda}^+ + \tilde{A}_{22}\tilde{\lambda}^- + \tilde{u}_0/\chi, \\
\tilde{A}_1 &= \tilde{u}_0, \\
\tilde{A}_{21}\mathrm{e}^{\tilde{\lambda}^+\xi_0^*} + \tilde{A}_{22}\mathrm{e}^{\tilde{\lambda}^-\xi_0^*} &= \tilde{A}_3\mathrm{e}^{\tilde{\lambda}^-\xi_0^*}, \\
\tilde{A}_{21}\tilde{\lambda}^+\mathrm{e}^{\tilde{\lambda}^+\xi_0^*} + \tilde{A}_{22}\tilde{\lambda}^-\mathrm{e}^{\tilde{\lambda}^-\xi_0^*} &= \tilde{A}_3\tilde{\lambda}^-\mathrm{e}^{\tilde{\lambda}^-\xi_0^*} + \tilde{u}_0^*/\chi^*, \\
\tilde{A}_3\mathrm{e}^{\tilde{\lambda}^-\xi_0^*} &= \tilde{u}_0^*,
\end{aligned} \qquad \text{(A.4)}$$

where $\chi = |du(0)/d\xi|$ and $\chi^* = |du(\xi_0^*)/d\xi|$. We must note here that one constant, $\tilde{u}_0$ or $\tilde{u}_0^*$, is determined by equation (A.4) and another one is arbitrary[6]. We choose $\tilde{u}_0$ as arbitrary constant. Eliminating $\tilde{u}_0$ and $\tilde{u}_0^*$ from the equations we compute the determinant of the matrix multiplying $(\tilde{A}_1, \tilde{A}_{21}, \tilde{A}_{22}, \tilde{A}_3)$,

$$\det \begin{pmatrix} 1 & -1 & -1 & 0 \\ \tilde{\lambda}^+ - 1/\chi & -\tilde{\lambda}^+ & -\tilde{\lambda}^- & 0 \\ 0 & \mathrm{e}^{\tilde{\lambda}^+\xi_0^*} & \mathrm{e}^{\tilde{\lambda}^-\xi_0^*} & -\mathrm{e}^{\tilde{\lambda}^-\xi_0^*} \\ 0 & \tilde{\lambda}^+\mathrm{e}^{\tilde{\lambda}^+\xi_0^*} & \tilde{\lambda}^-\mathrm{e}^{\tilde{\lambda}^-\xi_0^*} & -(\tilde{\lambda}^- + 1/\chi^*)\mathrm{e}^{\tilde{\lambda}^-\xi_0^*} \end{pmatrix} = 0 \qquad \text{(A.5)}$$

and obtain the growth rate relationship (3).

Finally we collect the expressions for the perturbation eigenfunction constants

$$\tilde{A}_1 = \tilde{u}_0, \qquad \text{(A.6)}$$

$$\tilde{A}_{21} = \frac{\tilde{u}_0}{\Omega\chi}(\Omega\chi - 1), \qquad \text{(A.7)}$$

$$\tilde{A}_{22} = \frac{\tilde{u}_0}{\Omega\chi}, \qquad \text{(A.8)}$$

$$\tilde{A}_3 = \frac{\tilde{u}_0}{\Omega\chi^* - 1}\frac{\chi^*}{\chi}. \qquad \text{(A.9)}$$

[6] However, this constant must be small because the perturbation Δu is small.

References

1. R. FitzHugh, Biophys. J. **1**, 445 (1961); J.S. Nagumo, S. Arimoto, S. Yoshizawa, Proc. IRE **50**, 2061 (1962)
2. R.A. Fisher, Ann. Eugenics **7**, 355 (1937)
3. A.N. Kolmogorov, I.G. Petrovskii, N.S. Piskunov, Bull. Univ. Moscow, Ser. Internat., Sect. A **1**, 1 (1937)
4. A.S. Mikhailov, *Foundations of Synergetics I. Distributed Active Systems* (Springer, Berlin, 1994)
5. M. Leda, A.L. Kawczyński, in *Proc. of the 3rd Eur. Interdisciplinary School on Nonlinear Dynamics EUROATTRACTOR 2003*, edited by W. Klonowski
6. H.P. McKean, Adv. Math. **4**, 209 (1970)
7. J. Rinzel, J.B. Keller, Biophys. J **13**, 1313 (1973)
8. J. Rinzel, D. Terman, SIAM J. Appl. Math. **42**, 1111 (1982)
9. A. Ito, T. Ohta, Phys. Rev. A **45**, 8374 (1992)
10. S. Koga, Physica D **84**, 148 (1995)
11. E.M. Kuznetsova, V.V. Osipov, Phys. Rev. E **51**, 148 (1995)
12. V. Méndez, J.E. Llebot, Phys. Rev. E **56**, 6557 (1997)
13. K.K. Manne, A.J. Hurd, V.M. Kenkre, Phys. Rev. E **61**, 4177 (2000)
14. R. Bakanas, Nonlinearity **16**, 313 (2003)
15. S. Theodorakis, Phys. Rev. D **60**, 125004 (1999)
16. J.-M. Roquejoffre, D. Terman, V.A. Volpert, SIAM J. Math. Anal. **27**, 1261 (1996)
17. S.A. Gourley, J. Math. Biol. **41**, 272 (2000)
18. E.P. Zemskov, Phys. Rev. E **69**, 036208 (2004)
19. M. Bode, Physica D **106**, 270 (1997)
20. A. Hagberg, E. Meron, I. Rubinstein, B. Zaltzman, Phys. Rev. E **55**, 366 (1997)
21. A. Prat, Y.-X. Li, Physica D **186**, 50 (2003)
22. E.M. Maslov, A.G. Shagalov, Physica D **152-153**, 769 (2001)
23. A. Hagberg, E. Meron, Chaos **4**, 477 (1994); A. Hagberg, E. Meron, Nonlinearity **7**, 805 (1994)